OPTIMAL VELOCITY MODEL WITH DUAL BOUNDARY OPTIMAL VELOCITY FUNCTION

Hao Wang[1,2]
[1]: Affiliation: School of Transportation, Southeast University
Address: 2, SiPaiLou, Nanjing, China, 210096
Phone: (+86) 13951920162
Email: haowang@seu.edu.cn
[2]: Affiliation: Department of Civil & Environmental Engineering, University of California, Davis
Address: 1, Shields Avenue, Davis, CA 95616
Phone: 530-304-1632
Email: tfcwang@ucdavis.edu

Abstract:

This paper proposes a Dual Boundary Optimal Velocity Model (DBOVM) by substituting a Dual Boundary Optimal Velocity Function (DBOVF) for the original one in the Optimal Velocity Model (OVM). The proposed DBOVM can describe the driving behavior of accepting a range of satisfied conditions instead of an optimal one under steady traffic. The speed adjustment mechanism is introduced into the DBOVM, by which traffic flow can reach the steady state everywhere inside of the dual boundary steady region. Properties of traffic state transition in the law of DBOVM are analyzed. The approximately linear path of state transition is found, and four typical state transition patterns are presented. Besides, the stability of DBOVM is studied by means of numerical simulations. It is found that the dual boundary steady region has the hysteresis effect that is similar to the explicit time delay in the OVM. The speed adjustment mechanism can restrain the hysteresis in some extent and improve the traffic stability. The dual boundary steady region in the general DBOVM allows the traffic flow to reach some new steady state slightly apart from the formal one under the effect of small perturbation, which does not exist for models containing one dimensional optimal velocity functions.

1 INTRODUCTION

Car following models, as one of the most useful tools for describing traffic dynamics, have been developed for more than six decades. There are two main objectives in the car following process: (i) reducing the speed difference and (ii) maintain an appropriate spacing between the following vehicle and the leading vehicle. Most early models as represented by GHR models were developed based on the first objective, but failed to describe the second one. Newell (1961) proposed a different model which successfully captures the characteristic of car following behaviors in maintaining an optimal spacing corresponding to the driving speed. However, due to the speed expression of Newell model, it is not convenient to be used in traffic simulations. Thirty years later, a new model called Optimal Velocity Model (OVM) was developed (Bando et al. 1995 & 1998). Similar to Newell model, the OVM contains the optimal velocity function, which allows the following vehicle to adjust its speed towards the optimal one, and consequently maintaining the appropriate spacing. Moreover, the OVM does not have a time delay in its model expression, which makes it convenient for theoretical analysis. Because of these advantages, the OVM has drawn widespread attention during the last twenty years (Helbing and Tilch 1999; Jiang et al. 2001).

The optimal velocity function assumes that there is a one-to-one correspondence between the spatial headway and the optimal driving speed in steady traffic state. However, such assumption may be too ideal from the driver's perspective (Boer 1999). Experience tells us that drivers are satisfied with a range of conditions instead of an accurate optimal performance. Actually, this fact was also noticed in some early studies related to the psychophysical or action point models (Brackstone and McDonald 1999). The action point models classify the driving conditions into several scenarios separated by threshold boundaries in the "spacing-relative speed" diagram. Drivers will not adopt acceleration or deceleration until the changes in conditions exceed the thresholds of drivers' perception. For instance, the Fritzsche model (Fritzsche 1994) and the Wiedemann model (Wiedemann and Reiter 1992) have a two-dimension zone in the "spacing-relative speed" diagram, within which drivers are satisfied with current conditions and maintain their speeds regardless of the performance of leading vehicles. Though the fundamentals of the action point model are closer to the real driving behaviors, the complexity of model structure and the difficulty in calibration of thresholds restrict its application in theoretical research areas.

Another question about the assumption of optimal velocity function in OVM came from the macroscopic observations of freeway traffic flow in recent years. Kerner and Rehborn (1996a & 1996b) first reported the widely scattered data of congested traffic in the fundamental diagram. Moreover, it was found that even the unstable data being removed, the remained steady traffic data still scatter in a two-dimension area in the flow-density plot. These empirical findings indicate that there might be an acceptable range of spacing within which drivers are satisfied. In order to model such phenomenon, several microscopic traffic flow models were developed in recent years (Kerner and Klenov 2002 & 2006; Davis 2004; Gao et al. 2009). Though solutions of steady state in these models occupy two-dimension areas, the numbers of parameters are more than the OVM, which increases the complexity of models and reduces the efficiency.

In this paper, a Dual Boundary Optimal Velocity Model (DBOVM) is proposed with the original optimal velocity function replaced by a Dual Boundary Optimal Velocity Function (DBOVF). The DBOVF is determined by two optimal velocity functions with different parameter values, which provides a range for spacing choosing in steady state. By introducing the DBOVF into the original OVM, the new model allows drivers to reach their steady states

within a wide region instead of a specific optimal solution. Besides, the DBOVM also shows some interesting properties different from the original OVM, which are also worthy of attention.

The rest of the paper is organized as follows. First, the basic DBOVM and a simple example of DBOVF are presented in section 2, and then stability analysis based on numerical simulation is conducted. In section 3, a more general form of DBOVM is proposed, and some related model properties are analyzed. Some results of comparison analysis between the DBOVM and the original OVM are also provided through numerical simulations. Finally, the possibility of model extension is discussed.

2 BASIC DUAL BOUNDARY OPTIMAL VELOCITY MODEL

2.1 The Model

Considering the facts that drivers would like to accept a range of spacing instead of an optimal one, we assume that the steady state occupies a two-dimension area in the speed-spacing diagram. As shown in Figure 1, there are two boundaries in the steady state region. Each boundary can be formulated by a certain type of optimal velocity function. The two boundaries of the steady state divide the speed-spacing diagram into three regions. In region Ⅰ, the spacing is too small for the driver to accept, and the driver will reduce the speed towards the optimal speed indicated by the left boundary optimal velocity function. In region Ⅲ, the spacing is too large, and the driver will accelerate towards the optimal speed indicated by the right boundary optimal velocity function. In region Ⅱ, the driver is satisfied with current conditions, and will not change the speed until the vehicle moves out of this steady region.

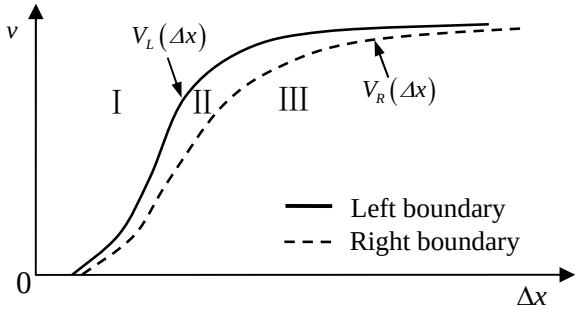

FIGURE 1 Illustration of dual boundary optimal velocity function.

According to above assumptions, the basic DBOVM is expressed as follows.

$$\ddot{x}_n(t)=\begin{cases}\kappa\left\{V_L(\Delta x_n)-\dot{x}_n(t)\right\} & if:\dot{x}_n(t)>V_L(\Delta x_n)\\ 0 & if:V_R(\Delta x_n)\le\dot{x}_n(t)\le V_L(\Delta x_n)\\ \kappa\left\{V_R(\Delta x_n)-\dot{x}_n(t)\right\} & if:\dot{x}_n(t)<V_R(\Delta x_n)\end{cases} \tag{1}$$

where $x_n(t)$ denotes the position of the *n*th vehicle, κ is the sensitivity parameter, $V_L(\Delta x_n)$ and $V_R(\Delta x_n)$ denote the optimal velocity functions of left boundary and right boundary respectively. The space headway is noted as $\Delta x_n(t)=x_{n-1}(t)-x_n(t)$.

2.2 Simple Example of Dual Boundary Optimal Velocity Function

Many types of optimal velocity functions were proposed during the history of traffic flow studies. Among them there are three typical types which were used most widely by researchers,

namely, the convex type represented by the exponential function (Newell 1961), the piecewise linear function represented by triangle fundamental diagram model (Daganzo 1994), and the S-shape function (Bando et al. 1995). In order to make comparison with the original OVM, we use the Bando's S-shape function as the boundary function to build the DBOVF. Before modeling the DBOVF, two requirements are considered as follows:

(i) The range of spacing in the steady state increases with the speed increasing;

(ii) For a given speed v_e, the smallest and largest spacing in steady state are $\Delta x_L = V_L^{-1}(v_e)$ and $\Delta x_R = V_R^{-1}(v_e)$, then the derivatives of the two boundary-optimal-velocity-functions at Δx_L and Δx_R should satisfy the following inequation $V_L'(\Delta x_L) \geq V_R'(\Delta x_R)$.

The first requirement comes from the studies on psychophysical car following models (Michaels 1961; Evans and Rothery 1977). These studies indicated that drivers perceive spacing changes through changes on visual angle subtended by the vehicle ahead. Under such a concept, the range of spacing in steady state may also be perceived through a change on visual angel, which is supposed to be nearly stable for various driving speeds. As the visual angle approximates to the ratio of the vehicle width to the spacing and the spacing generally increases with the speed increasing, the range of spacing is positively correlated to the driving speed.

The second requirement is from the consideration that the deceleration is usually stronger than the acceleration at the margin of steady state. Suppose a vehicle moves a small distance δ away from the left boundary of steady state Δx_L, with the speed remaining as $v_e = V_L(\Delta x_L)$. Then, the deceleration a_{dec} according to the DBOVM is

$$a_{dec} = \kappa\left[V_L(\Delta x_L - \delta) - v_e\right] \tag{2}$$

Expanding Equation (2) at Δx_L and ignoring the higher order terms, we get

$$a_{dec} = -\kappa\delta V_L'(\Delta x_L) \tag{3}$$

When the vehicle moves a small distance δ away from the right boundary of steady state Δx_R, we similarly have the acceleration a_{acc} as

$$a_{acc} = \kappa\delta V_R'(\Delta x_R) \tag{4}$$

Therefore, the requirement of $V_L'(\Delta x_L) \geq V_R'(\Delta x_R)$ ensure the asymmetry between the acceleration and the deceleration, i.e. $|a_{dec}| \geq |a_{acc}|$.

The S-shape optimal velocity function used in Bando's work (1998) is given as

$$V(\Delta x) = V_1 + V_2 \tanh\left[C_1\Delta x - C_2\right] \tag{5}$$

where all parameters, V_1, V_2, C_1, C_2 are positive values. Based on the requirements discussed above, we build a simple DBOVF as follows.

$$V(\Delta x) = V_1 + V_2 \tanh\left[C_1\Delta x - C_2\right], \quad C_1 \in \left[C_{1R}, C_{1L}\right] \tag{6}$$

and the two boundary-optimal-velocity-functions are given by

$$\text{Left boundary:} \quad V_L(\Delta x) = V_1 + V_2 \tanh\left[C_{1L}\Delta x - C_2\right] \tag{6a}$$

$$\text{Right boundary:} \quad V_R(\Delta x) = V_1 + V_2 \tanh\left[C_{1R}\Delta x - C_2\right] \tag{6b}$$

The parameter C_1 in the original OVM is replaced by C_{1L} and C_{1R}, which correspond to the left boundary and the right boundary respectively. The proposed DBOVF has a very simple model

structure and satisfies all the requirements listed above. In the following parts of this section, we will use it together with Equation (1) as the basic DBOVM to explore the properties of the model.

2.3 Stability Features of the Basic DBOVM

As a multiphase car following model, the DBOVM does not have a uniform model expression, which makes it difficult for the analytical stability analysis. In view of this fact, we hereby use numerical simulations to study the stability features of the basic DBOVM.

2.3.1 Local Stability

Treiber and Kesting (2013) gave a detailed theoretical analysis on traffic stability in their recent book. It is pointed out that all time-continuous car-following models with a negative derivative of acceleration with respect to speed are unconditionally locally stable, if there are no explicit reaction times in models. Recall the dual-boundary-optimal-velocity-function displayed in Figure 1, the basic DBOVM satisfies the criterion suggested by Treiber and Kesting when the local traffic state is located outside of the dual boundary steady region. However, as the driver does not perform any acceleration within the steady region, it delays the driver's response to the leading vehicle when the traffic state moves through the dual boundary region in the speed-spacing phase diagram. Therefore, the basic DBOVM is analogous to the OVM with explicit delay (Bando et al. 1998) in some extent. The simulation studies on the local stability of the basic DBOVM are as follows.

In order to make a comparison study, we use the same parameters as the early literature (Bando et al. 1998) used for the original OVM, namely, $V_1 = 15.3\,\text{m/s}, V_2 = 16.8\,\text{m/s}$, $C_1 = 0.086\,\text{m}^{-1}$, $C_2 = 2.1$, and $\kappa = 2.0\,\text{s}^{-1}$. For the basic DBOVM, we set $C_{1L} = 0.088\,\text{m}^{-1}$, $C_{1R} = 0.076\,\text{m}^{-1}$, and remain all the other parameters the same as in the original OVM.

Three vehicles are considered in the local stability studies. All vehicles are in steady state at the beginning of the simulation. For the studies on the basic DBOVM, the initial state of vehicles should satisfy either the left or the right boundary optimal velocity function. Otherwise, the following vehicles may not respond to the perturbation from the leading vehicle according to the law of the basic DBOVM. Therefore, three simulations are conducted for three different scenarios respectively, which are (ⅰ) initial state on the right boundary of steady region, (ⅱ) initial state on the left boundary of steady region, and (ⅲ) initial state satisfying the optimal function in original OVM. All three simulations begin with the driving speed of 10 m/s for all vehicles. Such a speed ensures that the initial condition satisfies the string stability criterion of the original OVM (Bando et al. 1995). Then a small perturbation is added on the leading vehicle by giving its position an instantaneous change (either increasing by 1 m or reducing by 1m). The simulations are conducted with the time step of 0.1 s, and results of the simulations are illustrated in Figure 2.

Let us first focus on the two subplots in the left side of Figure 2, which show the speed-headway phase diagram and speed time series of the simulation for the first scenario. Data of the first following vehicle and the second following vehicle are presented in red and blue respectively. The numbers of seconds counted from the beginning of the simulation are marked beside the data points in the phase diagram. Two black curves represent the left boundary and the right boundary of DBOVF respectively. At the beginning (t=0), both two following vehicles stay on the right boundary of steady region. The perturbation is added onto the leading vehicle at the first second. We can clearly see that the state points spiral counterclockwise towards the initial

steady state around the left and right boundaries. After 30 seconds, the two following vehicles are still unable to return to the initial steady state. Though the perturbation is quite small (less than 5% of the initial spacing), it is slightly amplified during it propagating upstream. We can find in the phase diagram that the blue state transition trajectory of the second vehicle is outside of the red trajectory of the first vehicle.

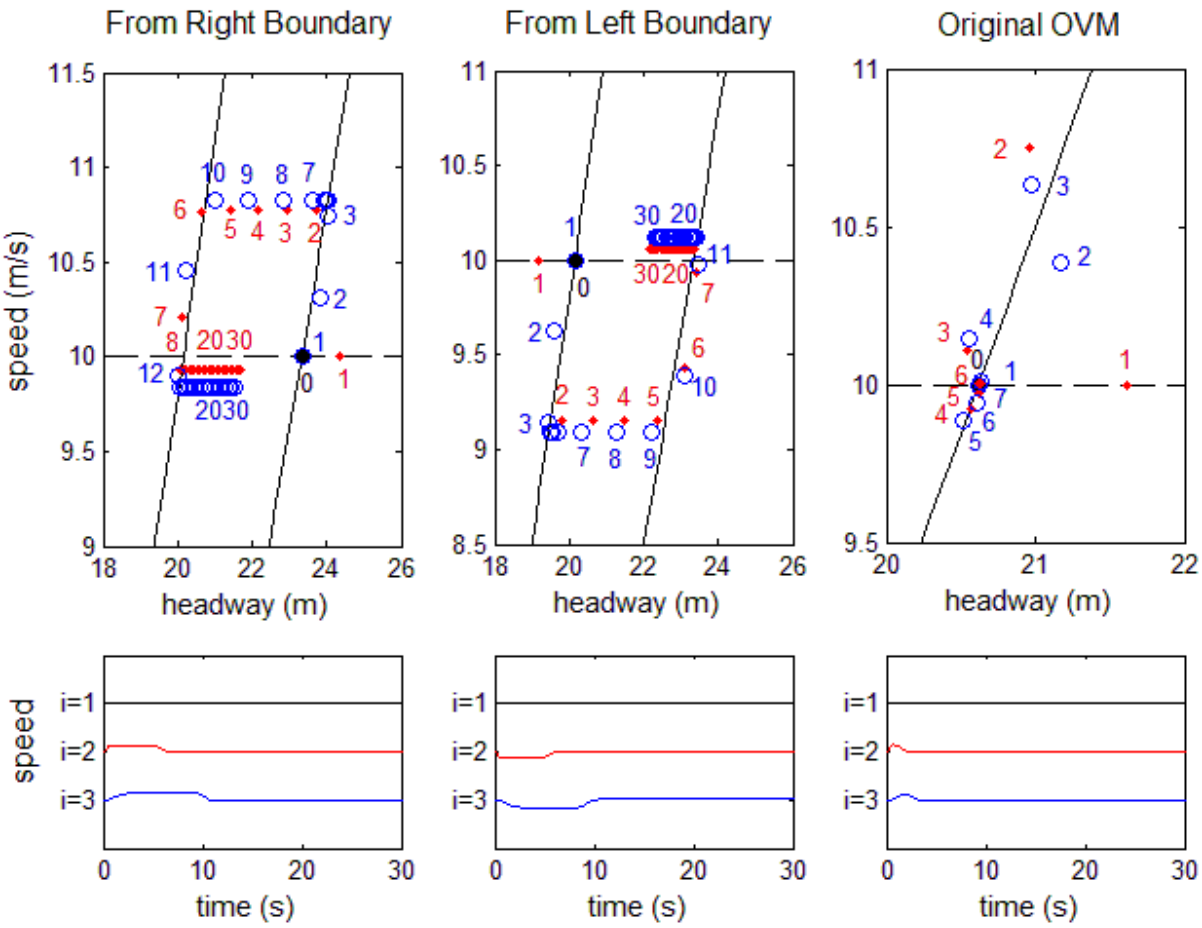

FIGURE 2 Phase diagram and speed time series of basic DBOVM.

In the second scenario, both two following vehicles stay on the left boundary of the steady region at the beginning. Similarly, the small perturbation is added onto the leading vehicle at the first second. The results of the simulation are displayed in the two subplots in the middle of Figure 2. We find the similar dynamical properties as shown in the first scenario. The states of the following vehicles move clockwise towards the initial steady state in a very slow manner. Moreover, the amplification of perturbation is also observed during it propagates upstream.

The two subplots in the right hand side of Figure 2 give the results of the simulation for the third scenario. Under the law of original OVM, the following vehicles return to the initial steady state much faster through smaller spiral trajectories. Both two following vehicles are found to recover to their initial steady state 6 seconds after the perturbation added.

Since the driver does not perform any acceleration in the two-dimension-region of steady state according to the basic DBOVM, it takes long time to converge to the steady state. Such

property may not have remarkable influence on the local stability of the basic DBOVM, whereas the slow convergence is likely to amplify the perturbation through the propagation. The following gives the simulation result of the dynamics of the basic DBOVM in a long platoon.

2.3.2 A Case of Perturbation Propagating along Platoon

We let all parameters remained the same as in the local stability studies. The platoon on the open boundary road involves 200 vehicles in the simulation. The initial speed and spacing are 5 m/s and 18.2 m for all vehicles in the platoon, which satisfies the right boundary optimal velocity function of the two-dimension-steady-region. Then the perturbation is added 10 seconds after the beginning of the simulation by giving the first vehicle's position a sudden increment of 1 meter. The time step is 0.1 s. The initial conditions above ensure the string stability for both two boundary optimal velocity functions under the law of original OVM (i.e. $V'(\Delta x) \le \kappa/2$). However, simulation for the basic DBOVM shows that the platoon is string unstable, as illustrated in Figure 3.

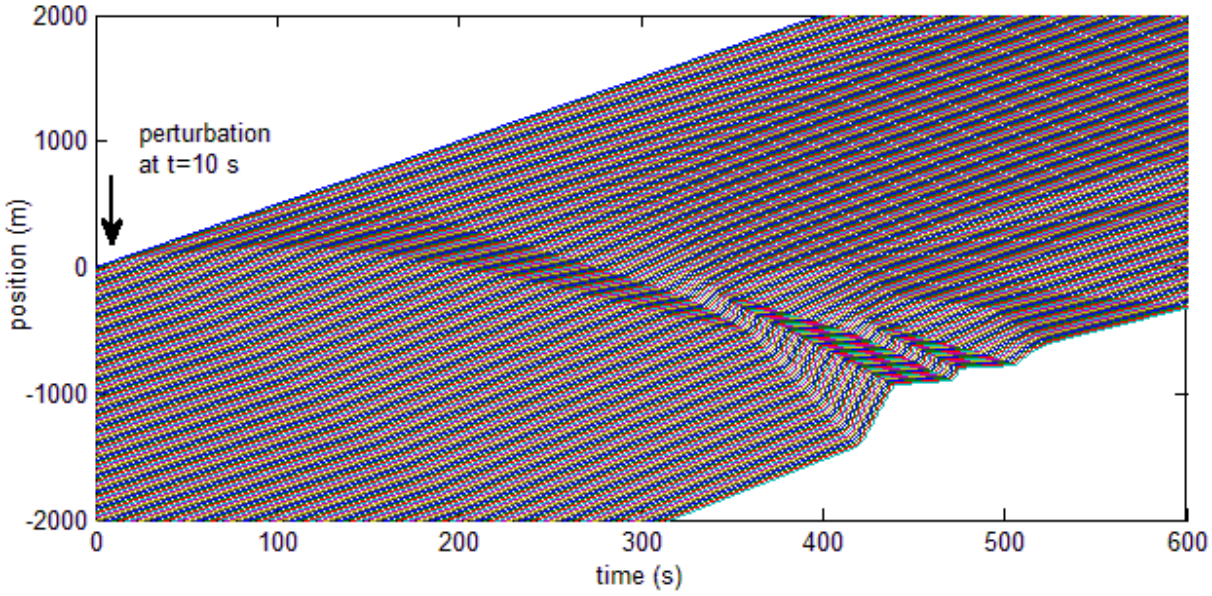

FIGURE 3 Propagation of small perturbation along the platoon in basic DBOVM.

A very slight acceleration wave can be found propagating upstream after the perturbation occurs. Then a deceleration wave appears followed by another acceleration wave. After about 360 s from the beginning, the deceleration wave merges into the following acceleration wave, which is again followed by a new deceleration wave. From Figure 3 we can clearly see that the small perturbation finally induces a stop-and-go wave during its propagation to the upstream of the platoon.

The simulation above indicates that the string stable criterion of the original OVM for the condition on boundary optimal velocity functions may not ensure the string stable of the basic DBOVM. In other words, the two-dimension-steady region in the basic DBOVM reduces the stability of traffic flow. The mechanism and some amendments about the model are given in the following parts of the paper.

3 GENERAL DUAL BOUNDARY OPTIMAL VELOCITY MODEL

3.1 The Model

In order to overcome the flaw in the basic DBOVM, we modify the model by introducing the speed adjustment mechanism into it. In the new model, drivers are allowed to adjust their driving speeds towards the speed of leading vehicles within the dual boundary steady region. The modified model is given below.

$$\ddot{x}_n(t)=\begin{cases}\kappa\left\{V_L\left(\Delta x_n\right)-\dot{x}_n(t)\right\} & if:\dot{x}_n(t)>V_L\left(\Delta x_n\right)\\ \lambda\left\{\dot{x}_{n-1}(t)-\dot{x}_n(t)\right\} & if:V_R\left(\Delta x_n\right)\le\dot{x}_n(t)\le V_L\left(\Delta x_n\right)\\ \kappa\left\{V_R\left(\Delta x_n\right)-\dot{x}_n(t)\right\} & if:\dot{x}_n(t)<V_R\left(\Delta x_n\right)\end{cases} \tag{7}$$

where λ is the sensitivity parameter of the speed difference between the leader and the follower. The speed adjustment mechanism captures the fact that drivers try to duplicate the speed of the vehicle ahead and maintain a stable spacing once they drive into their satisfied range of conditions, namely, the dual boundary steady region. As the basic DBOVM can be regarded as a special case of the new model ($\lambda=0$), we call the new model general DBOVM.

3.2 Properties of State Transition

According to the general DBOVM, the dynamic properties of vehicles are just the same as under the law of original OVM, when the traffic state locates outside of the dual boundary steady region in the speed-spacing diagram. In the following, the properties of state transition induced by the speed adjustment mechanism inside of the dual boundary region are analyzed.

3.2.1 Path of State Transition

Suppose the state of the *n*th vehicle is located inside of the dual boundary steady region at time t as shown in Figure 4(a). The speeds of the *n*th vehicle and the vehicle ahead are $\dot{x}_n(t)$ and $\dot{x}_{n-1}(t)$ respectively. According to the law of general DBOVM, the acceleration of the *n*th vehicle at time t is given by

$$\ddot{x}_n(t)=\lambda\left\{\dot{x}_{n-1}(t)-\dot{x}_n(t)\right\} \tag{8}$$

Assume that the vehicle moves with constant acceleration during a very small time interval τ, then speeds of the *n*th vehicle and (*n*-1)th vehicle at time $t+\tau$ can be expressed as

$$\dot{x}_n(t+\tau)=\dot{x}_n(t)+\tau\ddot{x}_n(t) \tag{9a}$$

$$\dot{x}_{n-1}(t+\tau)=\dot{x}_{n-1}(t)+\tau\ddot{x}_{n-1}(t) \tag{9b}$$

Then, the change of the spacing between the *n*th vehicle and (*n*-1)th vehicle during the time interval τ can be calculated as follows:

$$\Delta x_n(t+\tau)-\Delta x_n(t)=\tau\left\{\dot{x}_{n-1}(t)-\dot{x}_n(t)\right\}+\frac{\tau^2}{2}\left\{\ddot{x}_{n-1}(t)-\ddot{x}_n(t)\right\} \tag{10}$$

Therefore, the slope of the state transition path from time t to $t+\tau$ in the speed-spacing phase diagram can be derived as

$$\beta=\frac{\dot{x}_n(t+\tau)-\dot{x}_n(t)}{\Delta x_n(t+\tau)-\Delta x_n(t)} \tag{11}$$

By substituting Equations (8), (9a), (9b) and (10) into Equation (11), we finally get

$$\beta = \frac{1}{\frac{1}{\lambda} + \frac{\tau}{2}\left(\frac{\ddot{x}_{n-1}(t)}{\ddot{x}_n(t)} - 1\right)} \tag{12}$$

Equation (12) indicates that the slope β of the state transition path approximates to the sensitivity parameter λ in the general DBOVM when (i) the time step τ in the numerical calculation approaches zero or (ii) the following vehicle and the leading vehicle have similar accelerations. Specifically, when the speed of the leading vehicle remains stable (i.e. $\ddot{x}_{n-1}(t) = 0$), the slope of the state transition path is expressed as

$$\beta = \frac{1}{\frac{1}{\lambda} - \frac{\tau}{2}} \tag{13}$$

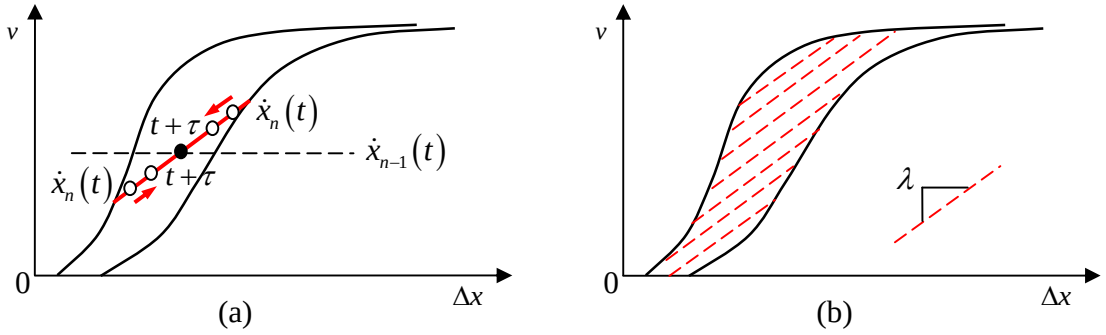

FIGURE 4 Paths of state transition within dual boundary steady region.

Considering that the time step used in numerical simulation for car following models is usually quite small (e.g. $\tau = 0.1$ s), the slope of the state transition path can be approximately expressed as λ everywhere within the dual-boundary-steady-region. As shown in Figure 4(b), the dual boundary steady region involves numerous parallel linear paths of state transition, as represented by the red lines in the figure. Once the traffic states reaches the boundaries of the steady region, the traffic states move along the state transition paths until converging at steady states. Figure 5 presents some simple scenarios of traffic states transitions in the speed-spacing phase diagram.

Suppose the leading vehicle's speed remains stable at $\dot{x}_{n-1}(t)$ during the traffic state transition of the following vehicle. The numbers in the figure denote the traffic states in terms of time series. The black solid dots represent the final steady states, which are always located at the horizontal line with the speed equal to $\dot{x}_{n-1}(t)$. Figure 5(a)-5(c) display the paths of state transitions from the start points (remarked by the number "1") to the final steady state (black solid dots). From Figure 5(a), we can find that the traffic state can converge to the steady state directly, if the initial state-transition-path along which the traffic state enters the dual-boundary-region has intersection point with the speed horizontal line of the leading vehicle. Otherwise, traffic state has to firstly move across the dual boundary region along the state-transition-path, and then spirals into the dual boundary region again to reach the final steady point (see Figure 5(b) and 5(c)).

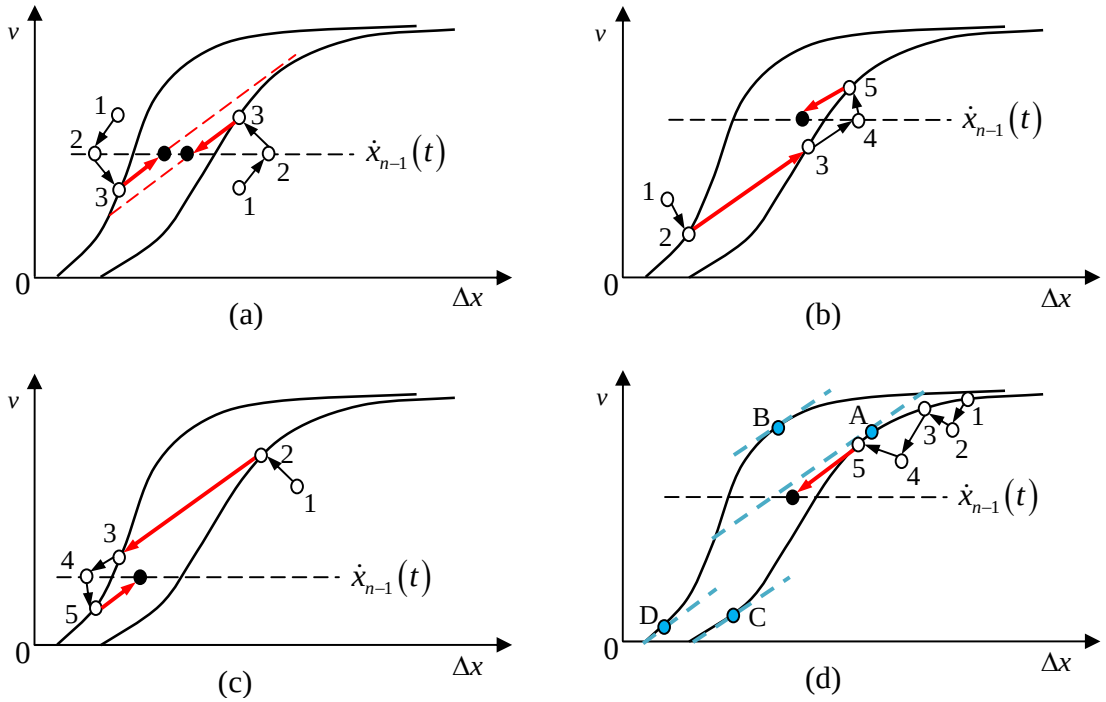

FIGURE 5 State transitions in speed-spacing phase diagram.

For most cases, there is at least one critical point on the boundary where the derivative equal to the slope of the state transition path. Figure 5(d) gives a special case, in which four critical points (point A, B, C, and D) exist on the two boundaries as represented by the blue solid dot. Let us take the critical point A for example. When the speed of leading vehicle is lower than that of the speed at point A, all the initial states that located in the right hand side of point A cannot find paths within the dual boundary region for state transitions. Instead, the state transition paths for such initial states go zigzag against the boundary until passing the critical point A, and then approach the final steady state along the state transition path. For the neighborhoods around other critical points, we can find similar properties of the state transitions, which are not necessary to go into details here.

3.2.2 Convergence of Traffic State

After obtaining the state transition paths within the dual boundary steady region, another interesting question is in what manner the traffic state moves along the state transition path. Suppose the *n*th vehicle reaches the right boundary of the two-dimension region at time t_0 in a deceleration process. The speeds of the *n*th vehicle and the vehicle ahead are denoted as $\dot{x}_n(t_0)$ and $\dot{x}_{n-1}(t_0)$, and we have $\dot{x}_n(t_0) > \dot{x}_{n-1}(t_0)$. For the sake of convenience, we assume that the leading vehicle keeps the speed $\dot{x}_{n-1}(t_0)$ stable. For a given time step τ, the speed of the *n*th vehicle at time $t_0+\tau$ can be derived according to model Equation (7) as follows:

$$\dot{x}_n(t_0+\tau) = \dot{x}_n(t_0) - \lambda\tau\left\{\dot{x}_n(t_0) - \dot{x}_{n-1}(t_0)\right\} \tag{14}$$

Similarly, the speed of the *n*th vehicle at time $t_0+m\tau$ is

$$\dot{x}_n\left(t_0+m\tau\right)=\dot{x}_n\left(t_0+\left(m-1\right)\tau\right)-\lambda\tau\left\{\dot{x}_n\left(t_0+\left(m-1\right)\tau\right)-\dot{x}_{n-1}\left(t_0+\left(m-1\right)\tau\right)\right\} \tag{15}$$

By recursive method, we obtain the solution of Equation (15) as

$$\dot{x}_n\left(t_0+m\tau\right)=\dot{x}_n\left(t_0\right)\left(1-\lambda\tau\right)^m-\dot{x}_{n-1}\left(t_0\right)\left\{\left(1-\lambda\tau\right)^m-1\right\} \tag{16}$$

Then, the speed difference between the *n*th vehicle and the vehicle ahead at time $t_0+m\tau$ can be expressed as

$$\Delta\dot{x}_n\left(t_0+m\tau\right)=\dot{x}_{n-1}\left(t_0\right)-\dot{x}_n\left(t_0+m\tau\right)=\left\{\dot{x}_{n-1}\left(t_0\right)-\dot{x}_n\left(t_0\right)\right\}\left(1-\lambda\tau\right)^m=\Delta\dot{x}_n\left(t_0\right)\left(1-\lambda\tau\right)^m \tag{17}$$

Equation (17) indicates that the speed difference between the following vehicle and the leading vehicle drops by $\left(1-\lambda\tau\right)$ in every time step. Specifically, the speed difference drops by $\left(1-\lambda\right)$ per second, when the time step τ equal to 1 second. If $\lambda=0.5\,\mathrm{s}^{-1}$, the speed difference drops by half per second, which also means that the distance between the current state and the final steady state along the state transition path is shortened by half every second as shown in Figure 6. Then, after 3 seconds, the speed difference drops to $1/8$ times of the initial value, and the following vehicle is approaching stable.

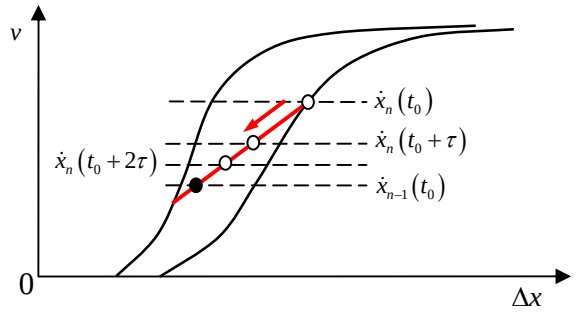

FIGURE 6 Process of state transition with $\lambda=0.5$.

Recalling the basic DBOVM proposed in Section 2, as the slope of the state transition path λ equal to zero, the speed difference cannot get any reduce during the state transition within the dual boundary steady region. That's why we find that the basic DBOVM always takes an unreasonable long time to approach the steady state. Moreover, the state transition paths in the basic DBOVM are horizontally distributed within the steady region, which indicates that the traffic state cannot reach the steady state theoretically. However, under the speed adjustment mechanism in general DBOVM, the traffic state can converge to any spacing in between the dual boundary steady region.

3.3 Stability Features of the General DBOVM

3.3.1 Local Stability

We use the same conditions as the studies on the basic DBOVM. Here the sensitivity parameter λ is set as $\lambda=0.5\,\mathrm{s}^{-1}$. Similarly to the studies in Section 2, two simulations are conducted, one for the initial state on right boundary and the other for left boundary. Figure 7 shows the simulation results of both scenarios. The red data and the blue data represent the first following vehicle and the second following vehicle respectively, and the numbers denote the time series of the state points. It is found that the slopes of all state transition paths are equal to

0.51 which is consistent with the result computed by Equation (13). As the time step of 0.1 s is used in the simulation, the rate of speed difference dropping per second can be computed by Equation (17) as $(1-0.5\times0.1)^{10}=0.60$. Therefore, in every second the speed difference drops to 0.60 times of it one second before, which is also consistent with the simulation results. After 6 seconds from the perturbation, the state of the first following vehicle is very close to the steady state. At the tenth second, the state of vehicle converges at some spacing in between of the two boundaries. Besides, it can be found that the final steady spacing of the second following vehicle is closer to the boundary in both scenarios, which proves that the effects of speed adjustment mechanism can allow the vehicle to reach any steady state within the dual boundary steady region.

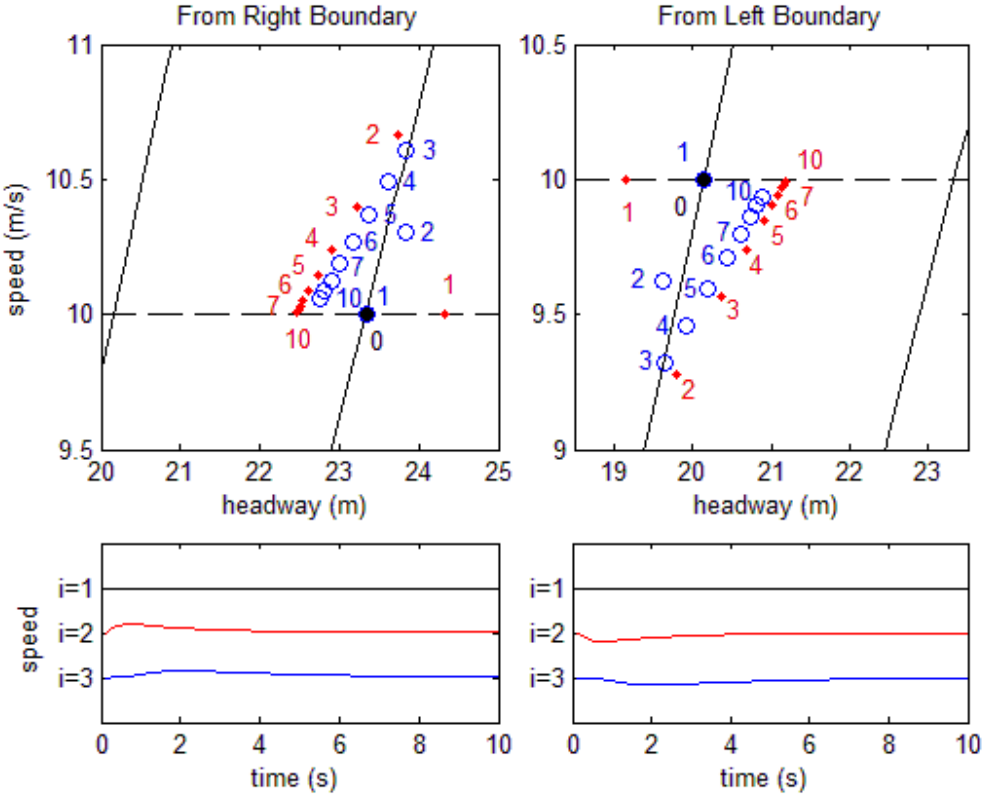

FIGURE 7 Simulations on local stability of general DBOVM.

The general DBOVM shows a similarity in the convergence speed with that of the original OVM, if one chooses an appropriate sensitivity parameter λ. In order to have deep insight of the dynamic features of the general DBOVM, numerical simulations on string stability studies are conducted in following.

3.3.2 String Stability

We use the periodical ring road as the simulation condition for studies on string stability. The platoon in the ring road involves 100 vehicles in total. Both the left boundary and the right boundary are considered as the initial steady state of the platoon in the ring. A small perturbation is added on the first vehicle by an instantaneous small jump (less than 5%) in position, and the time step is 0.1 s in all simulations. In order to make comparison, simulations are conducted for

all three models, i.e. original OVM, basic DBOVM ($\lambda = 0$), and general DBOVM ($\lambda = 0.5$). All model parameters are remained the same as in the local stability studies.

We first investigate the dynamics of the platoon under the unstable conditions. The initial speed of the platoon is 16 m/s, which is sting unstable for both the left boundary and the right boundary under the law of OVM. Figure 8 gives the snapshots of the platoon's dynamics at the time $t = 5000$ s from the time $t = 0$ at which the perturbation added. From the figure we can see that all three models produce the stop-and-go patterns after 5000 s. The hysteresis loop produced by the basic DBOVM is the largest in the phase diagram. With the effect of speed adjustment mechanism, the hysteresis loop of the general DBOVM is smaller, whereas the original OVM has the smallest one. Another feature needed to notice is the relation of the hysteresis loops between the original OVM and the basic DBOVM. In the simulation beginning from the left boundary of steady region, the left side of the hysteresis loop produced by OVM overlaps the same side of the DBOVM's loop, while they overlap in the right side for the case from the right boundary.

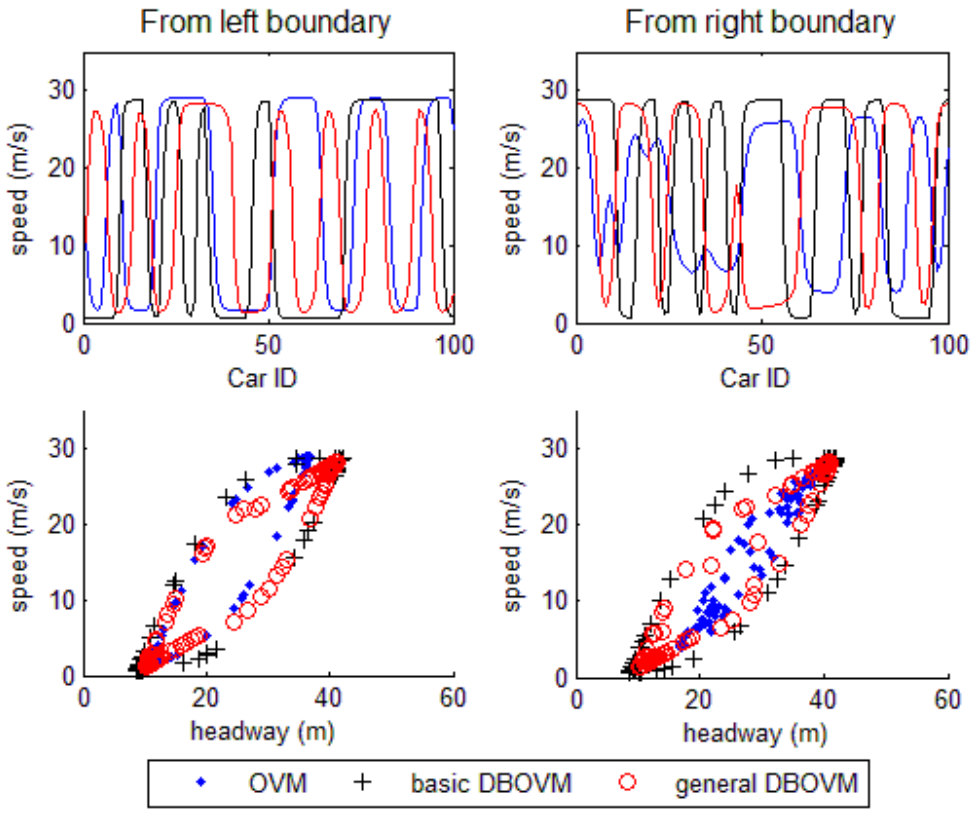

FIGURE 8 Snapshots of phase diagrams of three models at *t*=5000 s.

The simulation results indicate that the dual boundary steady region in the DBOVM has similar effect as the explicit delay for the original OVM (Bando et al. 1998), which can enlarge the hysteresis loop in traffic dynamics. However, the speed adjustment mechanism in the general DBOVM restrains such effect in some extent.

In the next step, we repeat the ring road simulation for every different initial steady state on the dual boundary (by the interval of 0.1 m/s in the initial speed), and add the total simulation

time to 100000 s, in order to ensure that the perturbation has sufficient time for evaluation. By trial and error, we get the string unstable region for the general DBOVM and the basic DBOVM as shown in Table 1.

TABLE 1 String Unstable Regions in General DBOVM and Basic DBOVM

	Left Boundary OVF $V(\Delta x) = 15.3 + 16.8\tanh[0.088\Delta x - 2.1]$	Right Boundary OVF $V(\Delta x) = 15.3 + 16.8\tanh[0.076\Delta x - 2.1]$
DBOVM $\lambda = 0.5$	$\Delta x \in (17.9, 31.7)$	$\Delta x \in (21.1, 31.8)$
	$v \in (7.2, 25.3)$	$v \in (7.6, 20.5)$
DBOVM $\lambda = 0$	$\Delta x \in (14.3, 34.9)$	$\Delta x \in (15.4, 40.3)$
	$v \in (3.8, 27.9)$	$v \in (3.0, 27.8)$
OVM	$\Delta x \in (16.5, 31.2)$	$\Delta x \in (22.0, 35.2)$
	$v \in (5.7, 24.9)$	$v \in (8.5, 24.0)$

We find that the string unstable regions in the basic DBOVM ($\lambda = 0$) are wider than the original OVM, due to the hysteresis effect induced by the dual boundary region. However, the string unstable regions for general DBOVM ($\lambda = 0.5$) are close to that of the original OVM, under the effects of speed adjustment mechanism. Because only small perturbations are considered in the simulations, the states of vehicles always move around the boundary where they get started, as illustrated in Figure 5(a). Therefore, the string unstable regions of speed are not the same on the two boundaries, but related to the mathematical properties of the boundary optimal velocity function. Moreover, as the derivative of left boundary optimal velocity function is larger than that of the right boundary at the same speed, simulations starting from the left boundary are likely to produce stronger acceleration (or deceleration) than the cases beginning from the right boundary, which makes the left boundary less stable than the right one. Therefore, the unstable region of DBOVM on the left boundary is wider than that in the right boundary.

Another interesting phenomenon can be found is that the final steady states which the platoon reaches after the perturbation is slightly different from the original ones where the platoon gets started. Specifically, the speed of the final steady state is higher than the initial steady state in the order of 0.1 m/s, when the platoon starts from the right boundary. For the cases of starting from the left boundary, the final steady speed is found lower than the initial one also in the order of 0.1 m/s. The two-dimension-steady-region allows the platoon to transfer its steady state under the perturbation. Similar shifts can be observed on the steady spacing of the platoon, if the simulation is conducted in an open boundary road instead of the ring road.

4 DISCUSSIONS

The basic DBOVM substitute the two-dimension-steady-region for the optimal velocity function in OVM, which is reasonable for modeling the satisfaction range of steady state in car following. However, the basic DBOVM cannot reach the steady state inside of the dual boundary region during the dynamic process of traffic flow. Therefore, the amendment of the speed adjustment mechanism is necessary in the general DBOVM. The effect of speed adjustment in the proposed model is similar to the speed adaption concept in the literature (Kerner and Klenov, 2002), while the latter one is more complex in model structure. Besides, the general DBOVM

has some similarities with the FVDM (Jiang et al. 2001) which also has a speed difference term in the model. The speed adjustment effect in the general DBOVM only works within the dual boundary steady region, whereas the FVDM does not contain a two-dimension-steady-region, and the speed difference term always contributes to the acceleration.

In this paper, only the S-shape function is considered for the expressions of the DBOVF. The differences in the functions of DBOVF may change the stability conditions of the general DBOVM, whereas the properties of traffic state transitions are the same as discussed in this paper. Another point that should be mentioned is the paths of state transitions within the dual boundary steady region are not strictly but approximately linear. However, one can still use the sensitivity parameter λ as the slope of the state transition path for roughly analysis.

5 SUMMARIES

The main contribution of this paper is that we proposed a simple car following model called general Dual-Boundary-Optimal-Velocity-Model, which can describe the driving behavior of accepting a range of satisfied conditions instead of an optimal one under steady traffic. The model is developed based on the Optimal Velocity Model with only two additional parameters. Therefore, it is very convenient for both analytical and numerical analysis.

A simple speed adjustment mechanism is introduced into the basic DBOVM, with which traffic state can converge to steady state everywhere inside of the two boundary steady region. Under the effect of speed adjustment, traffic states are transferred along some specific paths with an approximately constant slope equal to the sensitivity parameter of the speed difference term in general DBOVM.

The dual boundary steady region in DBOVM has the hysteresis effect, which is similar to the effect of explicit delay in OVM. The wider the dual boundary steady region is, the stronger the hysteresis effect will be. In spite of the instability resulted from the hysteresis of dual boundary region, the speed adjustment effect in general DBOVM restrains the hysteresis and improves the stability of traffic.

The dual boundary steady region in the general DBOVM allows the traffic flow to reach a new steady state slightly apart from the formal one under the effect of small perturbation. This property does not exist in models with one dimensional optimal velocity functions.

We should mention that we only present the framework of general DBOVM, and such dual boundary steady region can also be introduced into other well known car following models. Moreover, the parameters of general DBOVM are required to be calibrated by real traffic flow data, and applications of the proposed model will be studied in the next step.

ACKNOWLEDGMENT

This work is supported by National Natural Science Foundation of China (Grant No.51008074). The author would like to extend grateful thanks to some anonymous reviewers for helping improve this paper.

REFERENCES

Bando, M., K. Hasebe, A. Nakayama, A. Shibata, and Y. Sugiyama, A Dynamical Model of Traffic Congestion and Numerical Simulation. *Physical Review E*, Vol. 51, No. 2, 1995, pp. 1035-1042.

Bando, M., K. Hasebe, K. Nakanishi, and A. Nakayama. Analysis of optimal velocity model with explicit delay. *Physical Review E,* Vol. 58, 1998, pp. 5429-5435.

Boer, E. R. Car Following from the Driver's Perspective. *Transportation Research F*, Vol. 2, 1999, pp. 201-206.

Brackstone, M. and M. McDonald. Car-following: A Historical Review. *Transportation Research F*, Vol. 2, 1999, pp. 181-196.

Daganzo, C. F. The Cell Transmission Model: A Dynamic Representation of Highway Traffic Consistent with the Hydrodynamic Theory. *Transportation Research B*, Vol. 28, No. 4, 1994, pp. 269-287.

Davis, L.C. Multilane Simulations of Traffic Phases. *Physical Review E*, Vol. 69, 2004, id. 016108.

Evans, L. and R. Rothery. Perceptual Thresholds in Car Following: A Recent Comparison. *Transportation Science*, Vol. 11, No. 1, 1977, pp. 60-72.

Fritzsche, H. T. A Model for Traffic Simulation. *Traffic Engineering and Control*, Vol. 35, No. 5, 1994, pp. 317-321.

Gao, K., R. Jiang, B. H. Wang, and Q.S.Wu. Discontinuous Transition from Free Flow to Synchronized Flow Induced by Short-range Intersection between Vehicles in a Three-phase Traffic flow model. *Physica A*, Vol. 388, 2009, pp. 3233-3243.

Helbing, D. and B. Tilch. Generalized Force Model of Traffic Dynamics. *Physical Review E*, Vol. 58, No. 1, 1998, pp. 133-138.

Jiang, R., Q. S. Wu, and Z. J. Zhu. Full Velocity Difference Model for Car-Following Theory. *Physical Review E*, Vol. 64, 2001, pp. 017101.

Kerner, B.S. and H. Rehborn. Experimental Features and Characteristics of Traffic Jams. *Physical Review E*, Vol. 53, 1996, pp. 1297-1300.

Kerner, B.S. and H. Rehborn. Experimental Properties of Complexity in Traffic Flow. *Physical Review E*, Vol. 53, 1996, pp. 4275-4278.

Kerner, B.S. and S.L. Klenov. A Microscopic Model for Phase Transitions in Traffic Flow. *Journal of Physics A*, Vol. 35, 2002, pp. 31-43.

Kerner, B.S. and S.L. Klenov. Deterministic Microscopic Three-phase Traffic Flow Models. *Journal of Physics A*, Vol. 39, 2006, pp. 1775-1809.

Michaels, R. M. Perceptual Factors in Car Following.In *Proceedings of International Symposium on the Theory of Road Traffic Flow*, 1963, pp. 44-59.

Newell, G. F. Nonlinear Effects in the Dynamics of Car Following. *Operation Research*, Vol. 9, No.2, 1961, pp. 209-229.

Treiber, M. and A. Kesting. *Traffic Flow Dynamics: Data, Models and Simulation*. Springer, Berlin, 2013.

Wiedemann, R. and U. Reiter. *Microscopic Traffic Simulation: the Simulation System MISSION, Background and Actual State*, CEC Project ICARUS (V1052), Final Report, Vol, 2, Appendix A. Brussels: CEC, 1992.